STYRELSEN FÖR

VINTERSJÖFARTSFORSKNING

WINTER NAVIGATION RESEARCH BOARD

Research Report No 131

Mikko Suominen

STUDY ON FRICTION COEFFICIENT CORRECTION FOR MODEL-SCALE RESISTANCE TESTING IN BRASH ICE CHANNEL

Finnish Transport and Communications Agency
Finnish Transport Infrastructure Agency
Finland

Swedish Maritime Administration
Swedish Transport Agency
Sweden

Talvimerenkulun tutkimusraportit — Winter Navigation Research Reports
ISSN 2342-4303
ISBN 978-952-311-907-9

FOREWORD

In this report no 130, the Winter Navigation Research Board presents the results of a research project on a study on friction coefficient correction for model-scale resistance testing in brash ice channel. The project investigates friction coefficient correction on model testing in soft model ice and in solid freshwater ice cubes. Investigation is performed for different bow forms, including vessels with open water optimized large buttock angles.

The Winter Navigation Research Board warmly thanks Mikko Suominen for this report.

Helsinki

March 2024

Ville Häyrynen

Finnish Transport and Communications Agency

Amund Lindberg

Swedish Maritime Administration

Helena Orädd

Finnish Transport Infrastructure Agency

Fredrik Hellsberg

Swedish Transport Agency

Aalto-yliopisto
Aalto-universitetet
Aalto University

Study on Friction Coefficient Correction for Model-Scale Resistance Testing in Brash Ice Channel

Mikko Suominen

Aalto-yliopisto
Aalto-universitetet
Aalto University

Author(s) Mikko Suominen

Title Study on Friction Coefficient Correction for Model-Scale Resistance Testing in Brash Ice Channel

Project Friction Coefficient Correction for Model-Scale Testing (FRICCO)

Version Control Original Manuscript

Date 31.12.2023 **Number of pages** 40 **Language** English

Abstract

The friction coefficient correction for model-scale testing in brash ice channel may have a significant impact on the power requirement for an ice class that is determined through model-scale testing. However, it is not clear how applicable the friction coefficient correction presented in the FSICR guidelines is for ships having a vertical open water optimized bow forms, or if the tests are conducted in a brash ice channel formed from solid ice cubes as suggested by recent research.

This report presents model-scale measurements in brash ice channel conducted in Aalto Ice and Wave Tank. The measurements included resistance tests with simplified hull forms and a ship model having different friction coefficients in brash ice channels made from common soft model ice and solid freshwater ice cubes. The tests suggest the friction coefficient correction given in the FSICR guidelines is applicable for hull forms having a vertical bow form (large buttock angle) when those are tested in typical (relatively soft) model ice. On contrary, in a case testing in brash ice is conducted with solid freshwater ice cubes, the friction coefficient correction given by the rules does not appear directly applicable and further research is needed.

Keywords Friction coefficient correction; Brash ice channel; Model-scale

Table of contents

1 Introduction

Winter navigation system in the Baltic Sea consist of 1) icebreakers assisting merchant vessels, 2) national maritime administrators (Finnish and Swedish) setting traffic restrictions and developing the ice class rules, and 3) ice going merchant vessels that have an ice class. To secure the efficiency of the system, Finnish-Swedish Ice Class Rules set a minimum requirement for the ship performance in ice to obtain an ice class. As the merchant vessels are designed to operate in icebreaker assistance, the rules request a ship acquiring an ice class to be able to maintain a five knots speed in an old brash ice channel which ice thickness is defined by the pursued ice class.

The minimum power requirement to achieve this performance can be determined with the formulation given by the rules (FSICR, 2021) or through model-scale tests following the guidelines given by the rules (FSICR, 2019). This work focuses on the power determination through model-scale testing. Due to the complex behaviour of ice and limited possibilities in maintaining all major properties of model-scale ice simultaneously, it is difficult to match the testing conditions exactly to the conditions set by the rules. Thus, the measured model-scale test results are corrected to represent the desired conditions.

FSICR presents a formula for the friction coefficient correction (FCC) for model-scale testing in a case the measured friction coefficient deviates from the target value of the rules ($\mu = 0.1$), see Appendix 4 in FSICR (2019). Depending on the deviation between the target and actual friction coefficient, the FCC can have a strong impact on the determined power. Thus, it may have a significant impact on the required power for a vessel to obtain an ice class based on FSICR. Sufficient power level is important for ensuring the efficiency of the transport operations and functionality of the winter navigation system, but excessive power requirements hinder the vessels to meet the sustainable development goals and regulations related to those, such as EEDI. Thus, correctly defined power requirements are important.

Assumedly, the correction should be related to the ratio of resistance components, i.e. what portion of the total resistance is affected by the change in friction. The primary resistance components and their relation to one another are affected by several factors like: the main dimensions and hull form of the vessel, hull surface (friction), speed, ice condition (level ice, brash ice etc.), etc. Relatively recent study indicated the FCC given in the current rule guidelines overestimates the correction (Rehman, 2022). Furthermore, a recent study suggests the traditionally applied Froude-Cauchy scaling methodology in model-scale testing might be suboptimal for testing in a brash ice channel with vessels having EEDI type of hull forms (Matala & Suominen, 2022). These studies highlight the need to study the current FCC for model-scale testing in a brash ice channel with scaled down ice properties, and to develop a new FCC for the new scaling methodology that utilize unscaled ice

properties that improvs the modelling of brash ice behaviour and the accuracy of the resistant measurements (Matala & Suominen, 2022).

The aim of this work is to define the FCC for model-scale testing in brash ice channel with scaled down properties for open water optimized vessels having vertical bow form, like EEDI type of vessels. Furthermore, the aim is to defined FCC for the proposed new scaling approach for model-scale testing in a brash ice channel with ice having unscaled strength properties (Matala & Suominen, 2023). The FCCs are defined through testing models having simplified hull forms of ships and different friction coefficients. The simplified hull forms account different shapes of the bow at the waterline (a blunt shape waterline with vertical stem, a wedge shape waterline with vertical stem, and a wedge shape waterline with a sloping stem angle enhancing submersion of ice). To determine the FCCs for different types of ice, the tests are to be conducted in traditional model ice having scaled down properties and in ice with unscaled strength properties.

2 Resistance in Old Brash Ice Channel

2.1 Ship-Ice Interaction and Resistance

When a ship operates in a loose old brash ice channel, the bow displaces the ice pieces that causes resistance related to hull-ice friction and displacement, see Figure 1. The related forces depend mainly on the shear strength of the brash ice column. In a case of large buttock angle, like in open water optimized vessels or EEDI type of vessels, the ice is displaced horizontally, and the ice accumulates on the sides of the vessel. In a case of ice going vessel with a small buttock angle, part of the ice in the channel is pushed aside, and the rest is submerged. The displaced ice travels along the hull causing frictional resistance that is related to the buoyancy force at the keel, and pressure at the side from the accumulated ice. In both cases, the magnitude of the resistance is related to the mass and volume of the ice, and the friction coefficient between the ship and ice.

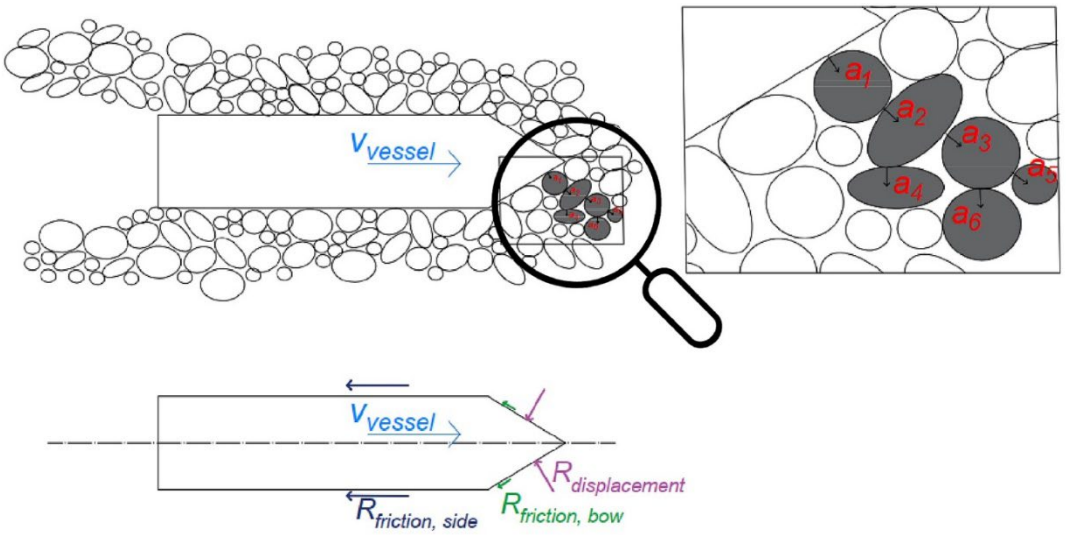

Figure 1. Ship-ice interaction and resistance in an old brash ice channel, modified from Matala and Suominen (2023).

A common approach to describe the brash ice resistance is to apply soil mechanics and describe brash ice as a Mohr-Coulomb type of material (Mellor, 1980). Following this approach and further applying Rankine's Theory, Riska et al (1997) developed a brash ice resistance calculation formulation that is the background for the rule formulation (FSICR, 2021).

$$R_{ch} = \frac{1}{2}\mu_B \rho_\Delta g H_F^2 K_p \left(\frac{1}{2} + \frac{H_M}{2H_F}\right)^2 \left[B + 2H_F\left(cos\delta - \frac{1}{tan\psi}\right)\right](\mu_h cos\varphi + sin\psi sin\alpha) + \mu_B \rho_\Delta g K_0 \mu_h L_{par} H_F^2 + \rho_\Delta g \left(\frac{LT}{B^2}\right)^3 H_M A_{WF} Fn^2 \quad (1)$$

where μ_B = 1-p and p is the porosity (μ_B = 0,8…0,9), ρ_Δ is the difference between water and ice density, g is the gravitational acceleration, K_P is the constant of passive stress (typically K_P = 6.5), H_M is the brash ice thickness in the mid channel, δ is the slope angle of the displaced ice against the ship side (22,6°), μ_H is the ship-ice friction coefficient, φ is the stem angle at the vertical at B/4, α is the waterline angle, K_o is the coefficient of lateral stress at rest (typically K_o = 0.27), L_{par} is the length of the parallel midbody at the waterline, A_{WF} is the waterline area of the foreship, and Fn is the Froude number. H_F is the thickness of the brash ice layer displaced by the bow aside that depends on the ship breadth, channel thickness and two slope angles that are dependent of the inner properties of brash ice. (Riska, 2014)

In a case B>10m and H_M>0.4m, H_F can be calculated from (Riska, 2014)

$$H_F = 0.26 + (BH_M)^{0.5} \quad (2)$$

and the flare angle ψ from

$$\psi = arctan\left(\frac{tan\varphi}{sin\alpha}\right) \quad (3)$$

2.2 Friction Coefficient Correction

FSICR (2019) assumes the superposition assumption is valid for the resistance. Thus, the total resistance, R_{TOT}, can be separated in pure ice resistance, R_i, and open water resistance, R_{ow}, as follows:

$$R_{TOT} = R_i + R_{ow} \quad (4)$$

In a case the resistance is determined through model-scale testing like a towed resistance test, the measured resistance is the total resistance. To correct the deviation between the testing and design conditions related to ice parameters, the pure ice resistance needs to be separated to target the corrections on it.

The friction coefficient, μ, ranges from 0.05 to 0.15 in full-scale whereas in model-scale testing the value is commonly between 0.05 and 0.1. Based on these, FSICR has set the design point of the friction coefficient to 0.1 (FSICR, 2019). In a case deviation occurs, the channel resistance, R_{ch}, can be corrected with the following formulation:

$$R_{CH(with\ \mu_{target})} = \frac{0.6+4\mu_{target}}{0.6+4\mu_{actual}} R_{CH(with\ \mu_{actual})} \quad (5)$$

where μ_{actual} is the friction coefficient measured in the tests, and μ_{target} is 0.1, i.e. the design value. Equation (5) could be interpreted in a manner that 0.6 of the total resistance is independent from friction, or 60 % of the resistance is independent from the frictional effects when the friction coefficient is 0.1.

According to Riska (2014), this correction was proposed by Keinonen et al. (1991). Keinonen et al. (1991) proposed the influence of friction on the ice resistance in full-scale can be estimated through temperature by first relating the friction coefficient to temperature, and then relating the effect of friction to resistance. Keinonen et al. (1991) noted that the influence on resistance can be estimated through theoretical calculation or model-scale tests. Furthermore, they presented summarized model-scale test results on the influence of friction coefficient on resistance in level ice with the friction coefficient correction. The model-scale tests had been conducted at the National Research Council in Newfoundland, Canada (Brown et al., 1988). The friction coefficient correction is presented in graphical format (Figure 11.4 in Keinonen et al., 1991), but it is obvious it has the form of Equation (5). Keinonen et al. (1991) note that the correction performs the best with hull forms where the buttock angles range from 20 to 25 degrees and flare angles from 45 to 60 degrees. These are more typical values for ice breaking ships than vessels designed for open water.

3 Measurement Methods for Ice Properties

3.1 Brash Ice Thickness Measurements

The brash ice thickness was measured prior tests with a measurement stick that had a tape measure attached to the side, and a handle lever that allowed to turn a perforated plate, attached to the stick with a joint, into a 90-degree angle, see Figure 2. The stick was pushed through the brash ice in straight orientation. Then the plate was turned with the lever in to 90-degree angle and lifted gently. While lifting, the surface of the brash ice was observed for movement indicating the plate had touched the keel of the brash ice. When a movement on the surface was observed, reading from the measurement stick was recorded. The thickness profiles from the channel cross-section were taken from three to five locations, depending on the width of the channel. The cross-sectional profiles were measured in two meters intervals along the length of the channel.

Figure 2. Ice thickness measurement stick with the perforated plate in straight and 90-degree angle orientation on the left and right, respectively.

3.2 Flexural Strength

The flexural strength of ice was determined through cantilever beam testing following the procedures described in ITTC (2021). The samples were cut from the model ice sheet with a milling drill bit connected to an electric drill. The electric drill was connected to the carriage system of the basin, which movements were controlled manually with the carriage positioning system (Petry et al., 2023). The target sample size followed ITTC (2021) guidelines, i.e., the length was five to seven times the thickness, and the width was two

times the thickness. The ice surrounding the free end of the beam was carefully removed to prevent possible interaction, see Figure 3. The indenter head used for loading was rounded around the width direction of the sample, had a joint allowing rotation around the length direction, and had a width half of a sample width, approximately. This system was considered to prevent the application of any torsion on the sample. The indenter contact line was approximately 1 cm from the tip of the sample.

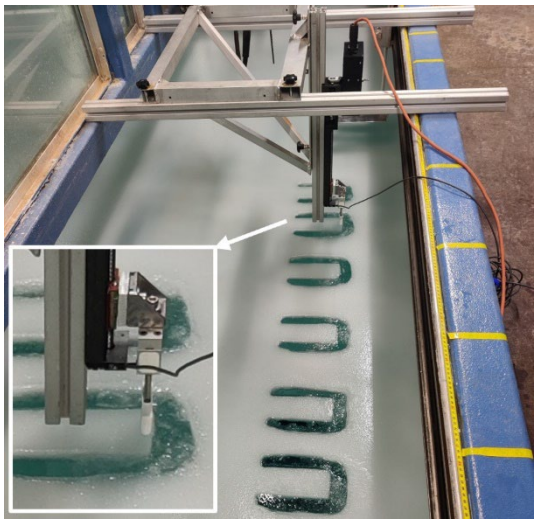

Figure 3. Cantilever beam testing setup for flexural strength measurement, modified from Petry et al. (2023).

Following the procedure, the flexural strength, σ_{flex}, can be calculated as

$$\sigma_{flex} = \frac{6Fl_b}{bh_i^2} \quad (6)$$

where, F is the measured force at the time of failure, l_b is the length from the loading point to the location of the crack, b is the width of the sample, and h_i is the ice thickness.

3.3 Friction Coefficient

Friction coefficients were measured on the side of Aalto Ice and Wave Tank in approximately zero-degree Celsius air temperature following the procedures described in ITTC (2021). A testing frame was placed on top of the model to be tested, see Figure 4. A rubber band was attached to the bottom of the frame that made the frame watertight from the testing area. After the frame was placed on top of the model, a thin layer of basin water from Aalto Ice and Wave Tank was poured inside the sealed area to have wet surface.

Before positioning an ice sample top surface down on the tested area, it was weighted with a letter scale. The dimensions of the samples were

approximately 20 cm * 20 cm * 3 cm (width * depth * height). After the sample was placed in the position, a plywood plate with a deadweight was positioned on top of it, see Figure 4. The plywood piece was used to distribute the pressure from the deadweight to prevent the failure of the sample. After the sample was in place with the additional weight, the sample was pushed through the testing area, approximately a distance of two meters, with an aluminium plate connected to an electric motor. The pushing force was measured with a load sensor from the aluminium pusher, see Figure 4.

Following this procedure, the friction coefficient can be determined as follows:

$$\mu = \frac{F_{meas}}{(m_{ice}+m_{plywood}+m_{weight})g} \quad (7)$$

where F_{meas} is the measured force, m_{ice}, $m_{plywood}$ and m_{weight} are the masses of ice, plywood, and deadweight used in the tests, respectively, and g is the gravitational acceleration. The model ice samples were extracted from model ice sheets produced for other tests. The freshwater samples for frictional measurements were grown from tap water in a freezer in a Styrofoam box.

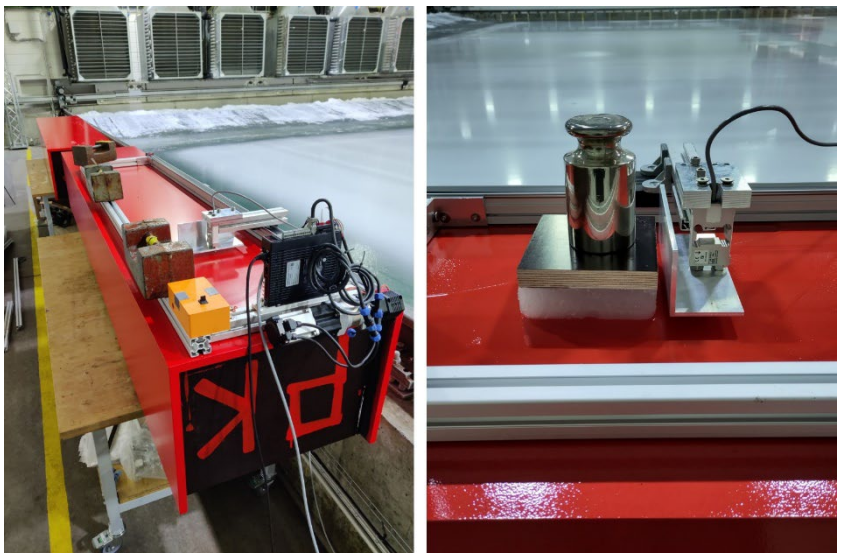

Figure 4. The general test setup applied in the friction coefficient measurements on the left and sample ready for testing on the right.

4 Test Preparations and Data Processing

4.1 Testing Facility and Model Ice Sheet

The measurements were conducted in Aalto University's Aalto Ice and Wave Tank. The basin is a 40 m by 40 m square basin, see Figure 5. The model ice sheet is produced through a spraying process where a fine mist of an aqueous solution doped with ethanol is sprayed in the air from a carriage moving over the basin. The sprayed solution lands on the surface of the basin, forming a thin layer of ice. This process is repeated until the desired ice thickness is reached, producing fine-grain model ice with grains of size equal to or smaller than one millimetre. Air temperature is kept below -10 to -15 ^{O}C during the spraying process and after the spraying to consolidate the formed ice. After the ice has consolidated, the air temperature in the basin is set to rise to obtain the desired strength level. In a case of brash ice test, the strength is not controlled, but a constant cold air temperature is kept. A detailed description of the procedures at Aalto University can be found in Jalonen and Ilves (1990).

Figure 5. Aalto Ice and Wave Tank, modified from Petry et al. (2023).

4.2 Brash Ice Channel Preparations

4.2.1 Model ice

Brash ice channels from model ice were produced from level ice sheets prepared as described in Chapter 4.1. When the brash ice channels were prepared, the goal was to apply procedures that could be repeated the same way for separate channels. Brash ice channels were prepared from level ice sheets having two target ice thicknesses, 20 mm and 30 mm.

The brash ice channels were prepared from 20 mm level ice sheet with a rotating hacking device, see Figure 6. The bottom part of the device has an

aluminium bar where corner brackets had been mounted in every 20 mm distance. The bar with the brackets was connected to an aluminium frame and a bevel gear. The aluminium frame was used to mount the device to the carriage, while the bevel gear enabled the rotation of the bar with an electric drill. In the channel preparation, the bar with the brackets was rotated with an electric drill while the carriage was driven through the basin. The bar chopped the ice sheet into cubes having a side length of 20 mm, approximately, see Figure 6. The carriage was driven over the basin until the desired width was achieved. While chopping the level ice, the device also mixed the brash ice. Thus, no further preparations were done for the channel prior thickness measurements and the actual tests.

Figure 6. Brash ice hacking device on the left. The device attached to the carriage on the top centre, and the bar with brackets chopping ice on the bottom centre. Prepared channel on the right.

The hacking device was applied to 35 mm level ice, but it had problems in chopping the ice. The device mainly did stripes or irregular sized large pieces. Thus, the device was not applied. A new cutting device consisting of knives was manufactured for the channel preparation, see Figure 7. The cutting device was attached to the carriage that was driven through the basin. This cut the sheet into 20 mm stripes. The stripes were hacked into smaller pieces utilizing an aluminium hacking device that had vertical plates used to break the stripes. After the hacking, no further actions were made to the channel, except the thickness was measured before the tests. Figure 8 presents a typical brash ice channel prepared from model ice before and after the tests. As can be noticed from the picture after the tests, model ice packs tightly and does not fill the channel after the model, as was noted in Matala & Suominen (2022).

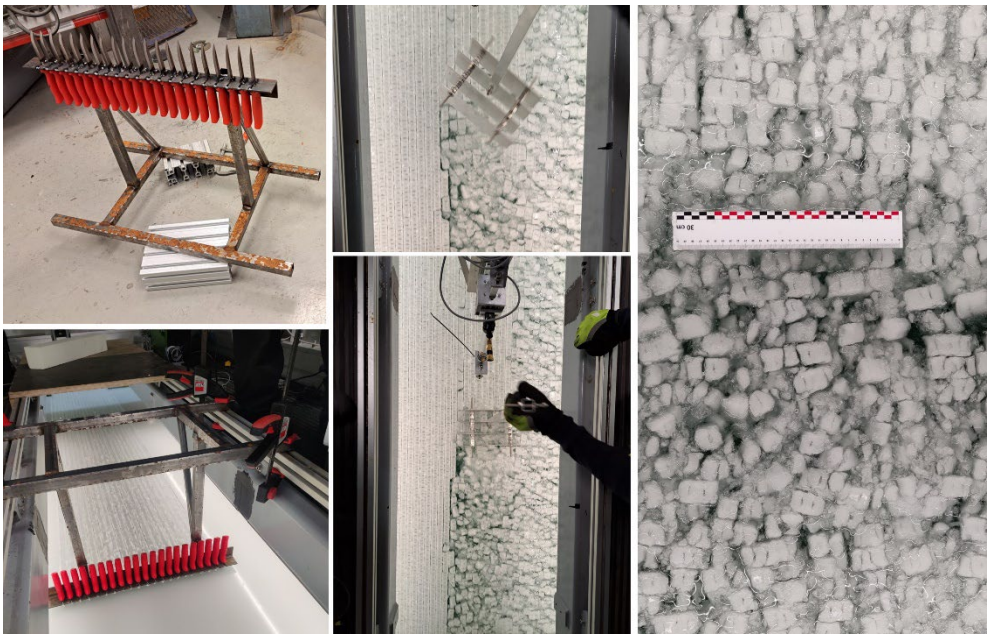

Figure 7. Setup used to cut the level ice into stripes, on the left, hacking device in operation in the centre, and the prepared brash ice channel.

Figure 8. A typical brash ice channel produced from model ice on the left, and the channel after the tests.

4.2.2 Ice Cubes

Brash ice channel made of freshwater ice cubes was made within model ice sheet. Approximately 35 mm thick model ice sheet was prepared following the procedure described in Chapter 4.2 without controlling the temperature. Channel edges were cut 1.2 meters apart (two times the breadth of the model having a simplified hull form) with the drill and drill bit used for mechanical property measurements. After the edges were cut, the ice between the edges

was cut into approximately 0.6 m times 1.5 m pieces that were pushed with a shovel under the ice surrounding the channel, see Figure 9. This was done to prevent the ice cubes escaping from the channel during the tests. Figure 10 shows the channel cleared from the ice that was submerge under the sides, note the whiter edges.

After the ice channel was prepared, it was filled with 4.8 m^3 of freshwater ice cubes. The ice cubes had a cylindrical shape and measured approximately 0.04 m in height and 0.015 m in radius, see Figure 11. The ice cubes were ordered from a commercial supplier. The ice arrived in separated boxes that were unpacked to large lifting bags that were lifted with a crane to the basin carriage and poured to the channel from the carriage. After all the cubes had been poured in the channel, a shovel was used to distribute the ice cubes more evenly along the length of the channel and control thickness measurements were taken, see Figure 10. The ice cubes behaved as described in Matala and Suominen (2022) and the channel closed right after the model, see Figure 12.

Figure 9. Channel preparation procedure for ice cubes.

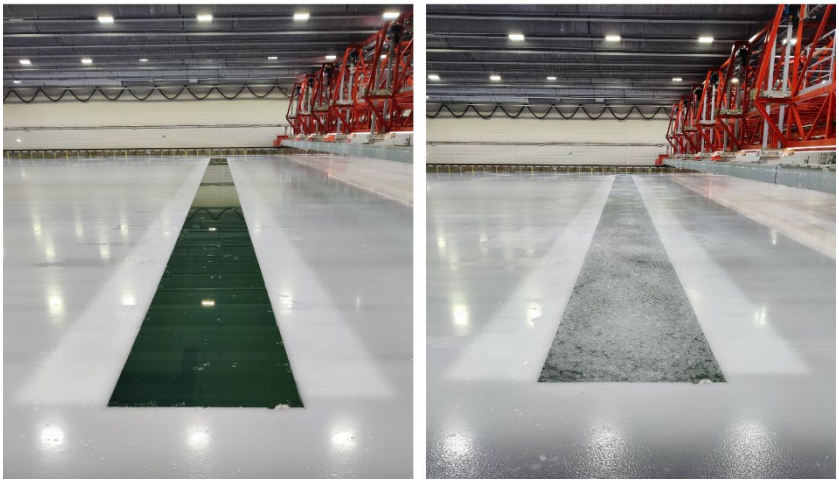

Figure 10. Open channel with ice submerged bellow the surrounding ice field on the left, and the channel filled with ice cubes on the right.

Figure 11. Ice cubes in the channel.

Figure 12. An ice cube channel before and after a test on the left and right, respectively.

4.3 Model Preparation

4.3.1 Simplified hull forms

The models were designed in ONSHAPE. Table 1 presents the main dimensions of the model and Figure 13 drawing of the model. MT Uikku was used as a reference ship in choosing the dimensions with a scaling factor of 30. The models were assembled from separate bow parts and parallel midship sections that were connected to each other with HBM single-point load sensors PW16AC3/30KG-1. Three types of bows were manufactured: 1) a bow having a vertical stem angle and a half circle waterline later referred as 'blunt', 2) a bow having a vertical stem angle and a wedge shape waterline later referred as 'wedge', and 3) a bow having a 50 degrees stem angle and a wedge shape waterline later referred as 'submerging wedge'.

Table 1. Main dimensions of the model.

Length	3.75m
Beam	0.6m
Draught	0.3m
Depth	0.45m
Bow Length	0.375m

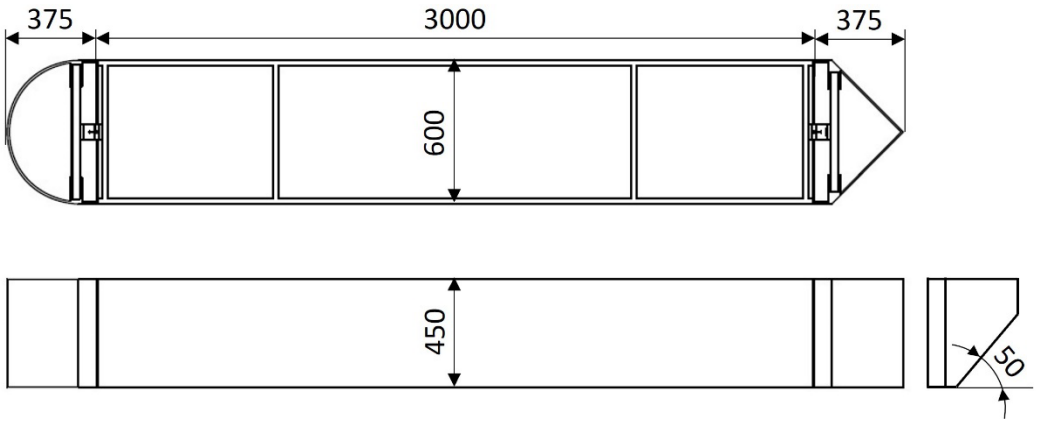

Figure 13. Model dimensions in millimetres.

The 50 degrees stem angle of the submerging bow started at the water line. Each bow part had a length of 0.375 m and a breadth of 0.6 m. The blunt and wedge bows were 3D printed in Aalto 3D printing facility with bigrepONE printer using polylactic acid (PLA), a common 3D printing filament. The front half of the bow models were printed using four lines creating a solid print with zero infill. The back half of the models were printed using two lines and 25% infill that made the structure slightly less rigid, but it reduced the print time and material usage. 34 mm thick plywood plates were attached with bolts to the printed bows to secure a rigid attachment for the load sensor, see Figure 14. The submerging bows and the parallel midsections were assembled from plywood parts with screws and glue. The unevenness of the outer surfaces of all the bows and midsections were smoothed with plaster and through sanding. Three pieces of each bow types and midsections were manufactured.

After the outer surfaces of the bows and midsections were smoothened, those were painted with an adhesive primer paint. Then paints having a different gloss level, half dim, half shiny, and shiny, as named by the producer, were used to paint the hull parts, see Figure 14. Each paint was applied to a piece of each bow type and a midsection. Different gloss levels were applied as a previous study had shown these to result in a different friction coefficient (Rehman, 2022).

The models were assembled for testing by attaching a bow part to a midsection part with a load sensor that was mounted at the water level. The load sensor was mounted on aluminium plates that were connected to the plywood plates attached to the hull parts, see Figure 14. Aluminium plates were applied between the load sensor and plywood to distribute the load. Duct tape was applied between the hull parts to prevent ice going between the parts. Figure 14 and Figure 15 present examples from assemblies. The models were assembled from hull parts having the same paint. In each model setup, one of the bow parts acted as the bow and one of the available bow parts as the stern, see Figure 15.

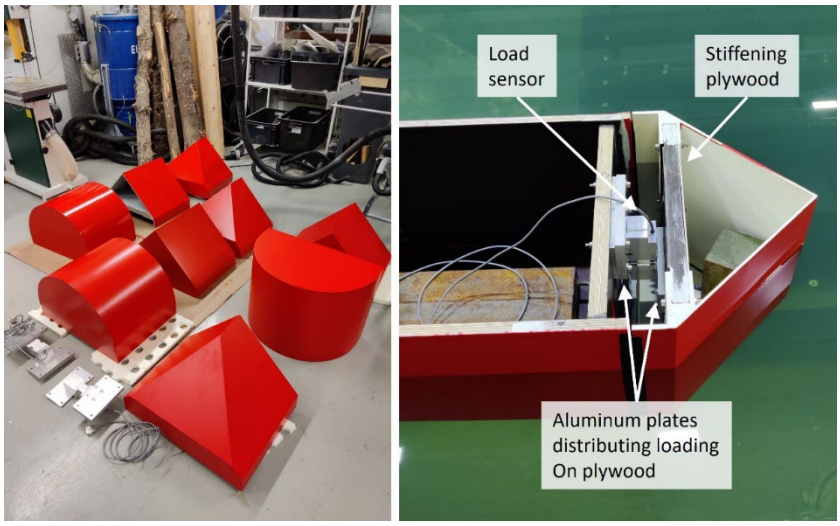

Figure 14. Finished bows and bow assembly on the left and right, respectively.


Figure 15. An assembled model.

4.3.2 Ship model

Testing with a ship model utilized the ship model developed and constructed in INFUTURE project, later referred as Infuture. Infuture is a double-acting general cargo vessel that is designed to break 0.6m level ice with speed of 2 knots astern (Li et al., 2021). The main dimensions of the ship are presented in Table 2. The applied scaling factor was 16.8.

To alter the friction coefficient of the model hull, the hull area below the waterline was covered with a shiny black D-C-fix contact plastic, see Figure 16. The contact plastic was mounted smoothly on the flat areas, areas having curvature in one direction, and areas having a modest curvature on one direction. Some unevenness could not be avoided in the areas having curvature

in two directions and joints. However, the portion of these areas from the total area was minor and these did not exist at waterline. Thus, the impact of these on the test results is considered negligible.

Table 2. Main dimensions of MT Infuture model.

Length overall	5.51 m
Breadth	0.750 m
Draught	0.264 m

Figure 16. Infuture covered with D-C-fix contact plastic.

4.4 Test Setup

The tests were conducted as towed resistance tests. For the test, the tested model was attached to the carriage moving under the bridge with a towing post. In a case of the simplified hull forms, the towing post was attached to the bulkhead of the model at the waterline through a HBM load sensor SP8-100KG, and a pneumatic damper, see Figure 17. The damper was applied to damp the possible oscillation at the start of a test run.

In a case of the ship model, the same type of test setup was applied as with the simplified hull forms. As a difference, the connection to the model was made with a stiffened corner bracket. The orientation of the ship model was controlled with guiding posts at the bow and stern that prevented sway, and yaw motions, but allowed surge, heave, pitch, and roll motions.

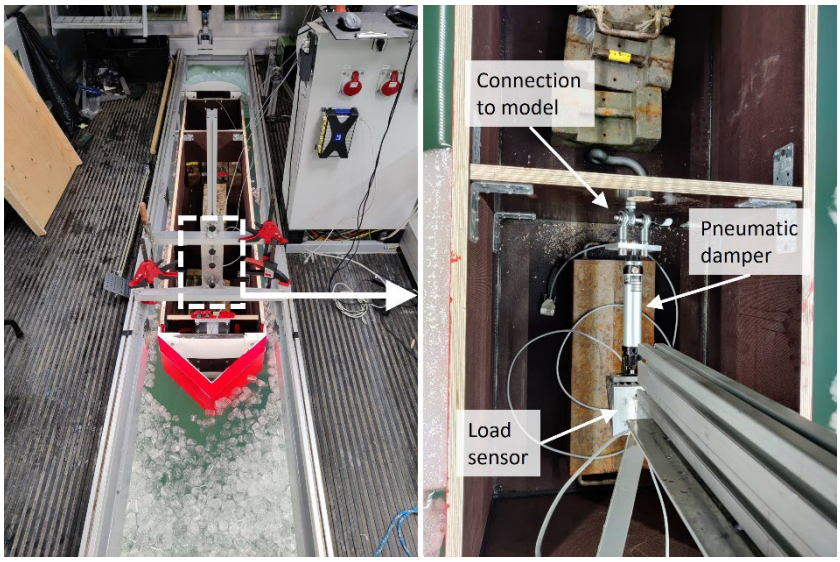

Figure 17. Test setup.

4.5 Data Recording and Processing

The measured signals included the towing force (i.e. the total resistance), the force between the bow and the parallel midship (i.e. the force acting on the bow), and the force between the stern and the parallel midship (i.e. the force acting at the stern part). The measurements were sampled with a frequency of 300 Hz using HBM QuantumX Data Acquisition System. A 50 Hz HBM Catman software build-in lowpass filter that had Bessel characteristics was applied to the data. No further filtering was applied to the data.

After the tests were conducted, steady states were searched from the measured towing force signal, i.e. a time frame where the force signal oscillated around a constant value, following the ITTC guidelines (ITTC, 2017). After the time frame with steady resistance was found, an average towing force was calculated from the period, and an average thickness was defined from the ice thickness measurements from the corresponding area, i.e. each obtained resistance measurement was related to ice thickness.

Although the brash ice channels were prepared following the same procedures in the same ice field, the measured ice thickness values had some variation between the tests. To study the effect of friction coefficient on the resistance, the thickness needs to be unified. Based on the ITTC guidelines (2017), the thickness correction can be applied to the measured resistance as follows

$$R_i = R_{i,meas}\left(\frac{h_{i,target}}{h_{i,meas}}\right)^x \quad (8)$$

where $R_{i,meas}$ is the measured resistance, $h_{i,target}$ is the target ice thickness, $h_{i,meas}$ is the measured ice thickness, and x is the correctional exponent that typically varies between 1.0 and 2.0. The exponent can be calculated based

on measurements in different thicknesses and is commonly defined based on the experience of the basin. However, the simplified hull forms with vertical lines and the tests with the ice cubes deviate from the common tests conducted in Aalto Ice and Wave Tank. For this reason, it was considered that the experience may not directly applicable for these tests and value of 1.5 was chosen for the data analysis. This was in balance between conservative and nonconservative values for thickness correction. However, the applied corrections were minor. Thus, the impact is considered small if other values would have been applied.

5 Results

5.1 Test Series

Table 3 summarises the conducted tests. In Test Condition column in Table 3: BI and OW indicate test in brash ice and open water, respectively; CX indicates the order (X) of the prepared channel; and Y1-Y2 indicate the location of the model bow in the beginning of the test (Y1), and at the end of the test (Y2). In Model Hull column in Table 3: Simp refers to tests with models having simplified hull form, and Infuture testing with the ship model; W, B, and SW refers to the applied simplified bow forms wedge, blunt, and submerging wedge, respectively.

Table 3. Summary of conducted tests.

Series	Date	Test No.	Test Condition	Model Hull	Model Surface
Test Series 1 - Model ice, ice sheet 20 mm	Nov 1, 2023	1.1	BI C1, 2-16	Simp W-B	Half dim
		1.2	BI C1, 16-32	Simp B-W	Half dim
		1.3	BI C2, 2-16	Simp W-B	Half shiny
		1.4	BI C2, 16-32	Simp B-W	Half shiny
		1.5	BI C3, 2-16	Simp W-B	Shiny
		1.6	BI C3, 16-32	Simp B-W	Shiny
Test Series 2, Ice cubes	Nov 22, 2023	2.1	BI C1, 2-32	Simp W-B	Shiny
		2.2	BI C1, 32-2	Simp B-W	Shiny
		2.3	BI C1, 2-32	Simp SW-B	Shiny
		2.4	BI C1, 2-32	Simp W-B	Half shiny
		2.5	BI C1, 32-2	Simp B-W	Half shiny
		2.6	BI C1, 2-32	Simp SW-B	Half shiny
	Nov 23, 2023	2.7	BI C1, 2-32	Simp W-B	Half dim
		2.8	BI C1, 32-2	Simp B-W	Half dim
		2.9	BI C1, 2-32	Simp SW-B	Half dim
Test Series 3, Ice cubes	Nov 24, 2023	3.1	BI C2, 2-32	Infuture, astern	D-C-fix
		3.2	BI C2, 32-2	Infuture, ahead	D-C-fix
		3.3	BI C2, 2-32	Infuture, astern	Paint
		3.4	BI C2, 32-2	Infuture, ahead	Paint

Seris	Date	Test No.	Test Condition	Model Hull	Model Surface
Test Series 4 - Model ice, ice sheet 35 mm	Dec 1, 2023	4.1	BI C1, 2-16	Simp B-SW	Shiny
		4.2	BI C1, 16-32	Simp SW-B	Shiny
		4.3	OW C0, 2-32	Simp B-SW	Shiny
		4.4	OW C0, 2-32	Simp SW-B	Shiny
		4.5	BI C2, 2-16	Simp W-B	Shiny
		4.6	OW C0, 2-32	Simp W-B	Shiny
		4.7	BI C2, 16-32	Simp B-SW	Half shiny
		4.8	OW C0, 2-32	Simp B-SW	Half shiny
		4.9	OW C0, 2-32	Simp SW-B	Half shiny
		4.10	BI C3, 2-16	Simp SW-B	Half shiny
		4.11	BI C3, 16-32	Simp W-B	Half shiny
		4.12	OW C0, 2-32	Simp W-B	Half shiny
	Dec 5, 2023	4.13	BI C1, 2-32	Simp SW-B	Half dim
		4.14	OW C0, 2-32	Simp SW-B	Half dim
		4.15	BI C2, 2-32	Simp B-SW	Half dim
		4.16	OW C0, 2-32	Simp B-SW	Half dim
		4.17	OW C0, 2-32	Simp W-B	Half dim
		4.18	BI C3, 2-32	Simp W-B	Half dim

5.2 Friction Measurements

Friction measurements were conducted as described in Chapter 3.3. The results with model ice and freshwater are presented in Table 4 and Table 5, respectively. To check possible effect of speed, testing location, and testing direction, these were varied between the tests. In addition, test repeatability was tested. It was concluded that these did not have a significant impact. Thus, an average was taken from all the tests with each tested paint or D-C-fix, see Table 4 and Table 5. It was noticed that the measured friction coefficient changes during the first tests in each test set, but then stabilizes. Thus, three first tests from each measurement set were neglected from the calculation of the average value for each test set.

Table 4. Measured friction coefficients with model ice.

Paint	Shiny				Half shiny				Half dim, side			Half dim			
Speed [mm/s]	100	100	50	100	100	100	50	100	100	100	50	100	100	50	100
Direction	forw.	forw.	forw.	rev.	forw.	forw.	forw.	rev.	rev.	forw.	forw.	forw.	forw.	forw.	rev.
Test \ Series	Ice2	Ice3	Ice4	Ice5	Ice6	Ice7	Ice8	Ice9	Ice10	Ice11	Ice12	Ice13	Ice14	Ice15	Ice16
1	0.019	0.023	0.027	0.017	0.115	0.099	0.096	0.106	0.234	0.212	0.205	0.199	0.175	0.163	0.138
2	0.028	0.038	0.043	0.034	0.132	0.105	0.111	0.101	0.195	0.165	0.183	0.176	0.152	0.147	0.128
3	0.033	0.043	0.048	0.044	0.125	0.109	0.117	0.101	0.182	0.160	0.172	0.170	0.147	0.145	0.129
4	0.036	0.044	0.048	0.050	0.119	0.115	0.120	0.102	0.170	0.158	0.169	0.168	0.145	0.145	0.128
5	0.037	0.047	0.047	0.052	0.113	0.115	0.120	0.105	0.169	0.158	0.165	0.165	0.144	0.145	0.126
6	0.038	0.044	0.048	0.051	0.109	0.113	0.119	0.106	0.165	0.159	0.167	0.163	0.145	0.144	0.127
7	0.038	0.044	0.048	0.053	0.109	0.113	0.120	0.107	0.161	0.156	0.167	0.158	0.142	0.145	0.128
8	0.038	0.043	0.048	0.053	0.107	0.114	0.116	0.107	0.158	0.157	0.170	0.156	0.143	0.145	0.126
9	0.038	0.043	0.046	0.054	0.108	0.114	0.114	0.109	0.157	0.157	0.163	0.154	0.142	0.149	0.126
10	0.038	0.043	0.047	0.054	0.107	0.113	0.115	0.110	0.162	0.157	0.162	0.152	0.141	0.144	0.127
Average 7 last	0.038	0.044	0.048	0.053	0.11	0.11	0.12	0.11	0.16	0.16	0.17	0.16	0.14	0.15	0.13
Average	0.045				0.11				0.16			0.14			
												0.15			

Table 5. Measured friction coefficients with freshwater ice.

Paint	D-C-fix	Shiny	Half shiny	Half dim
Speed [mm/s]	100	100	100	100
Direction	forw.	forw.	forw.	forw.
Test \ Series	Ice2	Ice1	Ice5	Ice1
1	0.0037	0.029	0.114	0.188
2	0.0038	0.017	0.107	0.149
3	0.0031	0.014	0.101	0.135
4	0.0026	0.014	0.095	0.131
5	0.0023	0.014	0.091	0.133
6	0.0022	0.014	0.089	0.125
7	0.0021	0.013	0.087	0.122
8	0.0021	0.015	0.088	0.124
9	0.0023	0.015	0.087	0.120
10	0.0023	0.016	0.087	0.126
Average 7 last	0.0023	0.014	0.089	0.13

5.3 Influence of Friction in Model Ice

Test series 1 and 4 were conducted in model ice sheets where the level ice sheet and brash ice channels were produced as described in Chapter 4.1 and 4.2.1, respectively. The channels were produced from level ice sheets that had target ice thickness of 20 mm and 35 mm in series 1 and 4, respectively. The average flexural strengths measured following the procedure described in Chapter 3.2 were 89 kPa, 94 kPa, and 78 kPa in the morning of Nov 1, Dec 1, and Dec 5, respectively. As all the tests involved in Test Series 4 could not be conducted in one ice sheet, two model ice sheets were prepared, one for the tests on Dec 1, and one for the tests on Dec 5. All the tests were conducted with a speed of 0.47 m/s.

Table 6 and Table 7 present the results from the measurements in model brash ice channels obtained as described in Chapter 4.5. Table 8 presents the results from open water tests conducted with Test Series 4. In Table 6 to

Table 8, "Simplified hull X-Y" refers to the model where X denotes the shape of the bow and Y the shape of the stern section following the naming presented in Chapter 5.1. The pure ice resistance can be defined by subtracting the open water resistance as indicated in Equation (4), i.e. reducing the values presented in Table 8 from the values presented in Table 6 and Table 7. After the ice resistance had been determined for each test, thickness was corrected following the methodology presented in Chapter 4.5 and applying Equation (8). The target ice thickness was set to 65 mm for Tests Series 1, and to 80 mm for the Test Series 4. Figure 18 shows the corrected ice resistance for Test Series 1 and 4.

Table 6. Results from Test Series 1.

	Test Series 1 - Model ice, ice sheet 20 mm					
	Simplified hull W-B			Simplified hull B-W		
Towing [N]	24.14	22.34	21.02	24.15	21.42	19.47
Bow [N]	27.48	25.39	25.51	22.46	19.96	20.08
Stern [N]	2.86	3.14	3.77	0.75	1.44	2.38
hice [mm]	62	63	65	64	60	66
Friction [-]	0.152	0.112	0.045	0.152	0.112	0.045

Table 7. Results from Test Series 4.

	Test Series 4 - Model ice, ice sheet 35 mm								
	Simplified hull W-B			Simplified hull B-SW			Simplified hull SW-B		
Towing [N]	36.87	42.88	29.02	37.90	46.81	28.83	39.36	31.78	33.24
Bow [N]	35.15	41.25	32.59	28.92	26.42	20.00	30.78	25.52	24.63
Stern [N]	3.65	4.54	3.96	3.80	2.07	3.76	4.16	2.19	0.83
hice [mm]	79	80	91	77	87	85	78	79	88
Friction [-]	0.152	0.112	0.045	0.152	0.112	0.045	0.152	0.112	0.045

Table 8. Measured open water resistances.

	Open water								
	Simplified hull W-B			Simplified hull B-SW			Simplified hull SW-B		
Towing [N]	11.40	11.45	10.68	7.51	8.78	10.15	11.69	11.72	11.80
Bow [N]	18.27	17.13	18.60	8.39	5.55	8.83	15.07	15.94	11.80
Stern [N]	2.54	3.05	2.51	2.82	1.06	2.38	3.03	0.55	0.34

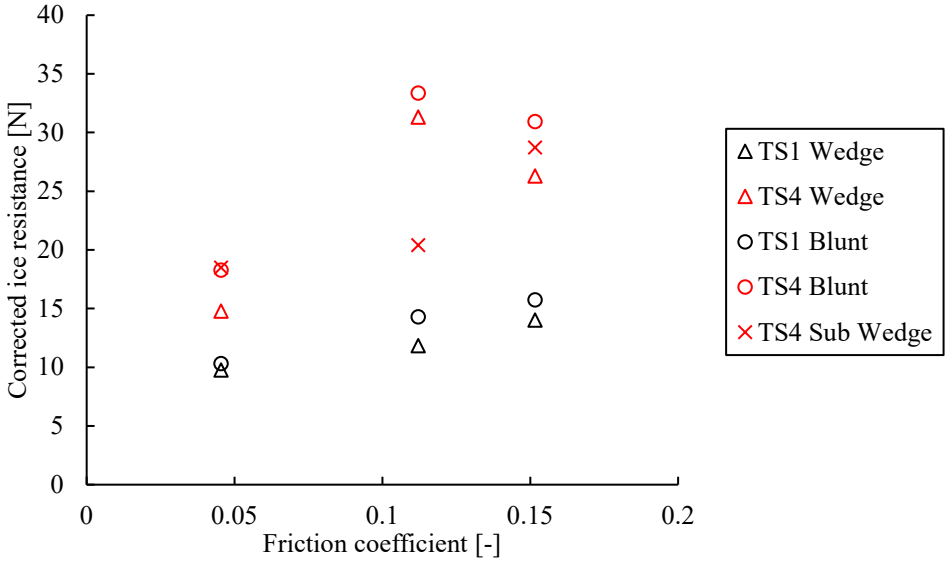

Figure 18. Corrected ice resistances for Test Series 1 and 4, referred as TS1 and TS4, respectively.

The results in Figure 18 show expected trends, i.e. the resistance increases as a function of friction coefficient, except the corrected ice resistance for the wedge and blunt bow in Test Series 4 with a friction coefficient of 0.112 (half shiny). The brash ice channel for the blunt bow (Test 4.7) was prepared well before the test as the model had to be changed between the tests 4.6 and 4.7. This could have affected the results as ice was broken in the basin water. The wait for the wedge was not as long but it could have had an impact. Due to the clear deviation, these points were considered as outliers.

Next, the corrected resistances were normalized for the resistance at friction 0.1. The resistances with friction coefficient were defined by fitting a linear trendline to each set presented in Figure 18 separately, and then calculating the ice resistance at friction coefficient 0.1. After the resistances for each set were defined at this point, the resistance values belonging to the set were divided with the resistance defined for the friction coefficient of 0.1. Note that outliers were not included when trendlines were determined. Figure 19 shows the normalized ice resistances. As can be noted, the values are closely in line, beside the outliers, and all the bow types show similar trend. Following this, the sets were combined and a trendline was fit to the combined data, see Figure 20. As can be noted, the form of the fitted trendline is close to the rule-based friction correction, see Equation (5).

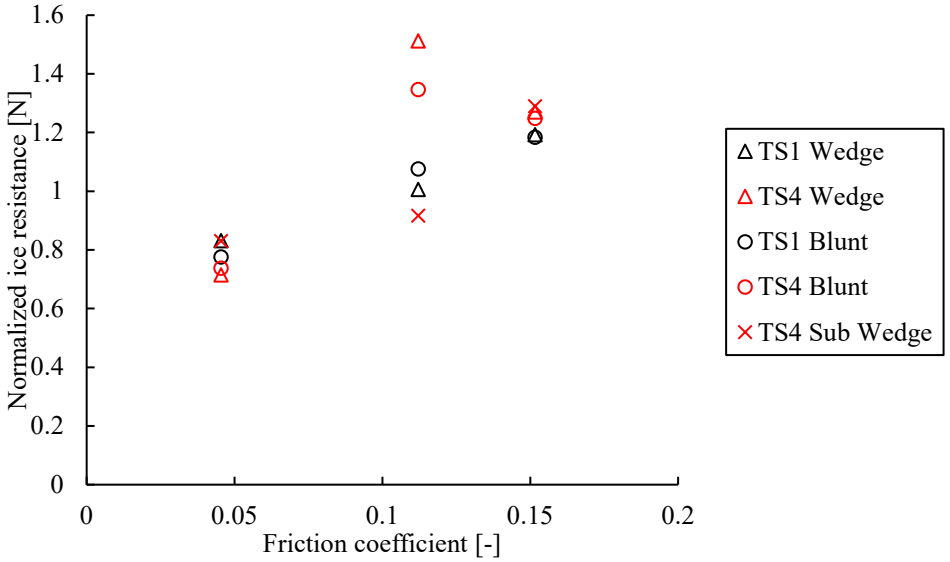

Figure 19. Normalized ice resistances for Test Series 1 and 4, referred as TS1 and TS4, respectively.

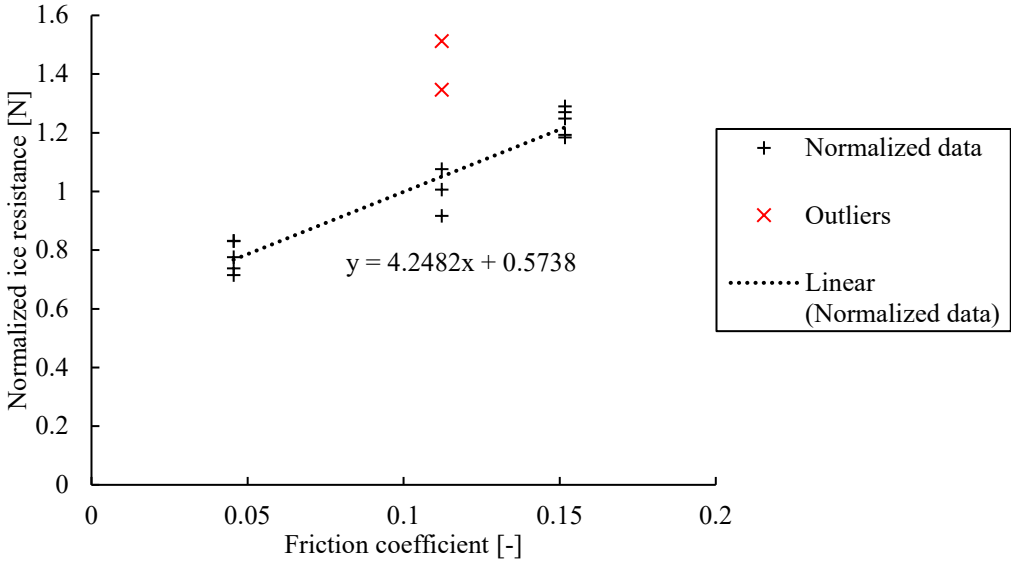

Figure 20. Trendline fitted to the normalized ice resistance values.

5.4 Resistance in Ice Cubes

Test Series 2 and 3 were conducted in brash ice channels made from fresh-water ice cubes. All the tests included in these series were conducted with the same ice cubes and with a speed of 0.47 m/s. The model ice sheet and the channel were produced as described in Chapter 4.1 and 4.2.2, respectively. The cubes were preserved overnight by keeping sub-zero air temperature in the basin area. In the following morning, the channel was hacked in a similar manner to model ice channels preparation to break the ice that had possibly

formed between the ice cubes. The channel prepared for series 2 was 1.2 m wide, i.e. two time the breadth of the simplified models, as recommended by the rules (FSICR, 2019). Before the series 3, the channel was widened to 1.5 m, i.e. two times the width of Infuture model. Open water tests with Infuture model were not included in the tests as those had been measured to be 4.61 N astern and 4.84 N ahead within other tests.

As a result of the channel preparation procedure and the length of the channel, it was challenging to obtain uniform ice thickness along the length. However, the test length allowed long measuring distance. Thus, two measurement points were obtained from each test run with models having simplified hull form. If the measured time history indicated change in resistance, the points were taken from the locations indicating different resistances. The results from Test Series 2 and 3 are presented in Table 9 and Table 10, respectively. Following the same procedure as in Table 6 to Table 8, "Simplified hull X-Y" refers to the model where X denotes the shape of the bow and Y the shape of the stern section following the naming presented in Chapter 5.1.

Table 9. Results from Test Series 2 with models having simplified hull forms.

	Test Series 2, Ice cubes											
	Simplified hull W-B						Simplified hull B-SW					
Towing [N]	48.78	60.52	45.14	33.77	43.23	36.03	41.26	44.83	39.38	45.36	34.18	33.80
Bow [N]	41.36	50.66	42.22	33.15	44.65	37.68	31.83	34.96	34.38	39.45	27.73	27.22
Stern [N]	4.35	4.33	4.64	4.39	4.09	3.94	3.13	3.84	2.40	2.41	2.61	2.69
hice [mm]	131	138	124	111	140	121	125	129	138	141	126	121
Friction [-]	0.126	0.126	0.089	0.089	0.014	0.014	0.126	0.126	0.089	0.089	0.014	0.014

	Simplified hull SW-B					
Towing [N]	46.94	44.66	44.17	33.20	35.59	28.74
Bow [N]	33.98	33.65	44.05	36.78	41.83	36.57
Stern [N]	1.64	1.62	4.33	3.89	-0.89	-1.15
hice [mm]	124	122	135	119	115	110
Friction [-]	0.126	0.126	0.089	0.089	0.014	0.014

Table 10. Results from Test Series 3 with Infuture model.

	Test Series 3, Ice cubes			
	Astern		Ahead	
Towing [N]	16.03	26.21	20.66	27.63
Bow [N]	122	118	122	115
Stern [N]	0.0023	0.041	0.0023	0.041

Following the same procedures as in Chapter 5.3, the ice resistances were first corrected for the same thickness and then the results were normalized, see Figure 21 and Figure 22 respectively. The thicknesses were corrected to a target thickness of 130 mm. The corrected and normalized ice resistance does

not show any clear outliers. Furthermore, the tested bow shapes appear to follow the same trend and the resistance do not show clear differences. However, commonly the resistance is considered to increase linearly as a function of the friction coefficient. The trend in Figure 21 and Figure 22 appears to be more of an exponential shape. However, fitting other forms of dependencies would require deeper understanding and further studies from this. Thus, a liner trendline was fitted to the data, see Figure 23. In this case, the trendline deviates from the equation proposed in the rules for friction correction, compare Figure 23 with Equation (5).

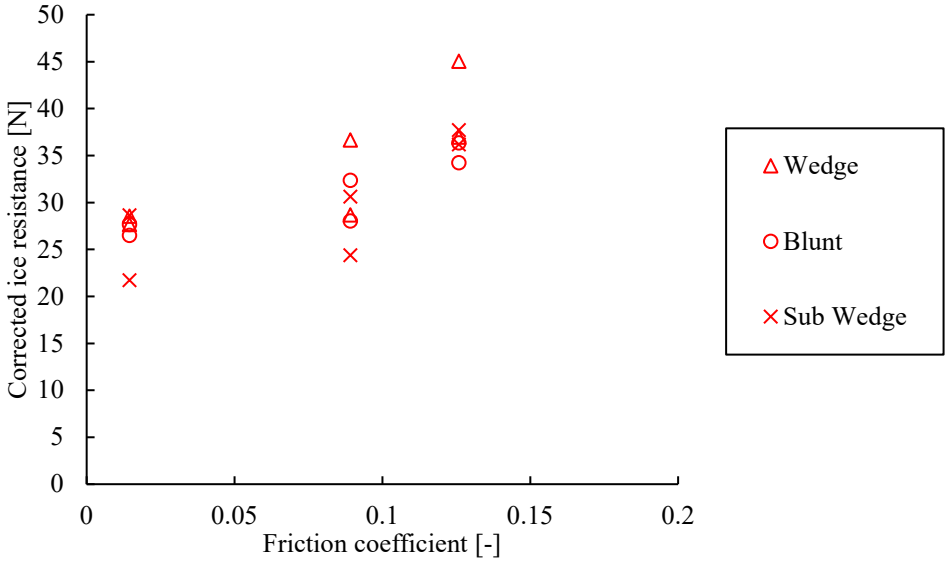

Figure 21. Corrected ice resistances for Test Series 2.

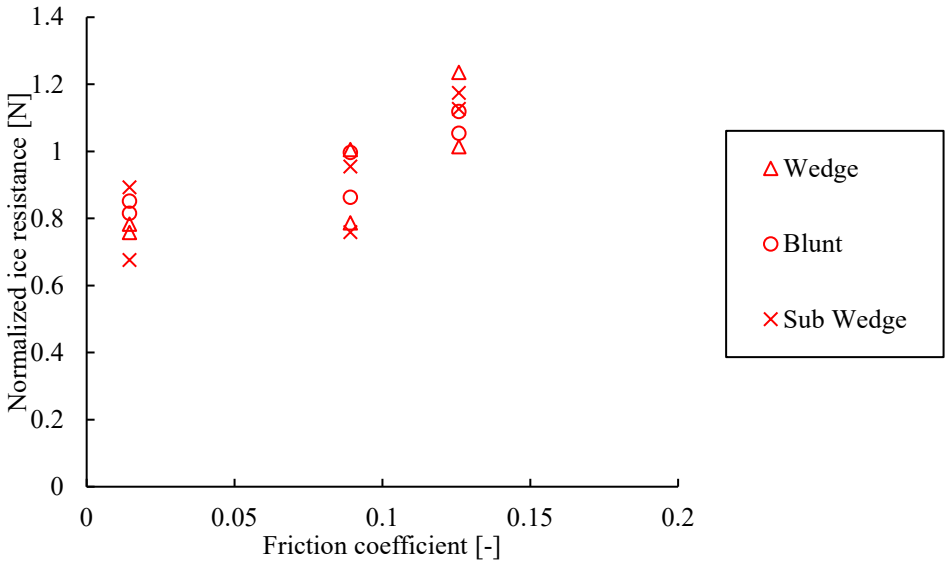

Figure 22. Normalized ice resistances for Test Series 2.

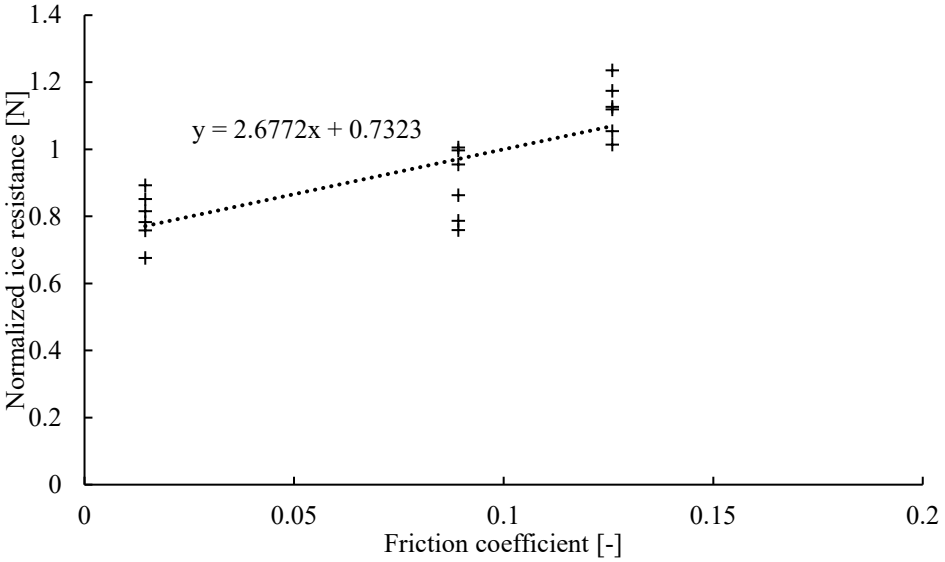

Figure 23. Trendline fitted to the normalized ice resistance values. Black line and equation are related to the whole data.

It should be noted that the results presented in Figure 21 to Figure 23 were obtained with simplified hull forms. To get better comparison, the same process was applied to the data obtained with Infuture model. In a case of Infuture, the ice thicknesses were corrected to a target thickness of 120 mm. Trendlines fitted to the normalized data are presented in Figure 24. As can be noted, the trendlines obtained from the fits to Infuture data deviate from the simplified hull form data. However, if the measurements with the simplified hull form models having the lowest friction coefficient are neglected, and the afore mentioned data processing is executed for the remaining of the data, the fitted trendline gives a good correspondence to the trend with Infuture measurements, see Figure 25. This would suggest a linear trend. However, it is difficult to draw definitive conclusions based on these findings. Further discussion can be found from Chapter 6.3.

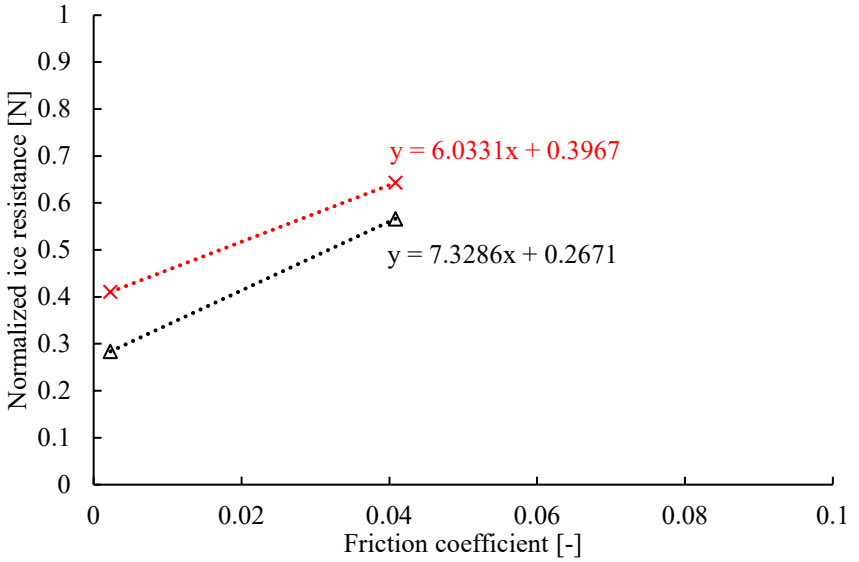

Figure 24. Trendlines fitted to the normalized data. The red colour indicates results related to tests ahead, and black colour results related to tests astern.

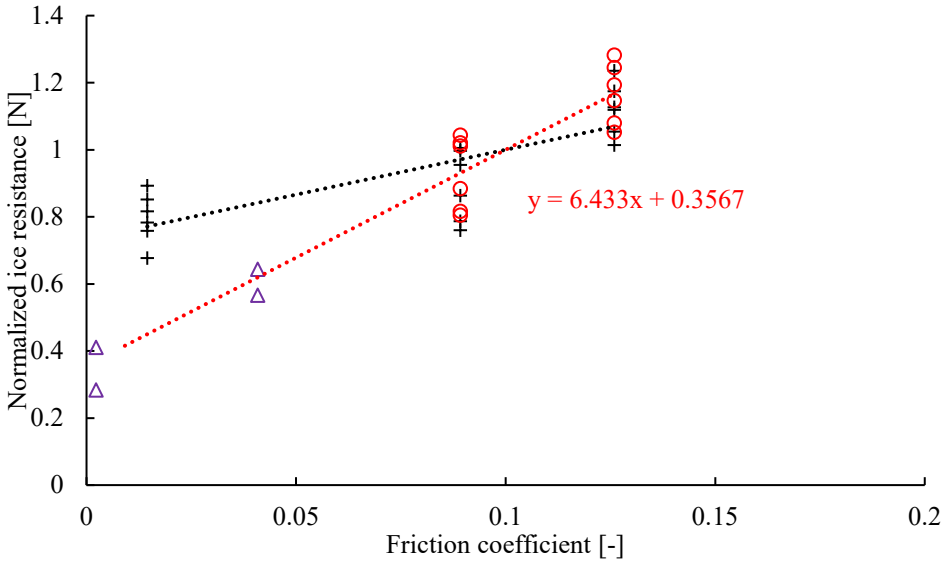

Figure 25. Trendline fitted to the normalized ice resistance values. Black markers are the data points for simplified hull forms when all the data is utilized. Red markers are measurements with simplified hull forms when the measurements with the lowest friction are neglected. Red line is the trendline fitted to the simplified hull form data when the values obtained with the smallest friction are neglected. Purple triangles are normalized ice resistances obtained from Infuture data.

6 Discussion

6.1 Resistance related to different hull areas

The results with simplified hull forms indicate that different bow waterline shapes have minor impact on the total resistance in brash ice channel made from model ice. Tests with freshwater ice cubes did not show any indication with simplified hull forms. However, tests with Infuture model suggested that resistance astern (small buttock angle, large waterline angle) is smaller than ahead (close to vertical buttock angle, smaller waterline angle) that would be in line with current knowledge.

Simplified hull forms were built from segments to study the resistance related to different hull areas. However, the measurements showed that the force measured in open water at the bow is larger than the towing force when wedge and submerging wedge is used as a bow. This is believed to relate hydrodynamic effects related to the relative sharp corners at the bow shoulder and sharp angles at keel. When the forces measured at open water conditions are reduced from the total forces, the towing forces are larger than forces at bow or stern in ice conditions. However, it appears that the local hydrodynamic effects are strong on these local areas, and the superposition assumption may be too significant simplification that requires further studies including hydrodynamics. Thus, forces at separated hull areas were not studied further, and the friction coefficient correction was not related to the main dimensions or ratios between the main dimensions of the hull.

6.2 Relation of Applied Speed, Thickness, and Scaling to FSICR Guidelines

Scaling was not discussed in this research as the focus was on the friction coefficient correction in model-scale testing in brash ice channel. The scaling factors were mentioned when the models were presented to indicate the approximate size of the considered vessels. If commonly applied Froude-Cauchy scaling would have been applied with the reported scaling factors, the testing speed with simplified hull forms would have been in accordance with the FSICR design conditions (5 knots), but the speed with Infuture would have been below (3.7 knots). Furthermore, the channel thicknesses would exceed the target ice thickness in the channel for any ice class.

These are believed not to have an impact on the application of the results. The applied speeds and ice thicknesses vary in model-scale testing based on the scaling factor. The used values are in line with the commonly applied values. Furthermore, as the study focused on the influence of friction coefficient to ice resistance, the effect of ice thickness was unified when the thickness was corrected for each set. In addition, after the speed and ice thickness were

constant for a set, the effect was taken out by normalizing the resistance to the resistance with a friction coefficient equalling 0.1. Here it is assumed that the difference in speed or thickness does not alter the interaction processes that is believed to be valid as the tests were done in common testing range.

6.3 Influence of Friction on Resistance in Ice Cube Channel

Definitive conclusions are difficult to draw for the friction coefficient correction for the resistance test in a brash ice channel made from freshwater ice cubes. The measurements with simplified hull forms suggest the influence of friction on ice resistance is non-linear. It is not clear where this could relate to, as friction is commonly considered to have a linear impact on ice resistance. One explanation could be that friction alters the processes around the ship hull. With lower friction, the ice moves smoother around the hull, especially at the bow. When the friction increases, ice pieces are not displaced as easily at bow, and ice compacts more in front of the bow. This alters the ice-ice interaction process at the bow region, especially with large buttock and waterline angles. This could explain the non-linear influence of friction with simplified hull forms.

In a case of bow having small buttock and/or waterline angle, like the Infuture model (a small buttock angle at stern and a small waterline angle at bow) the afore mentioned effect could be reduced. However, only two measurement points were obtained with Infuture model. Thus, it is not possible to study the possible non-linear trend. Furthermore, when the measurements with the simplified hull forms having the lowest friction coefficient are neglected, the results align well with the results obtained with the Infuture model. This observation does not support the above explanation for bow region, as this suggest the measurements with simplified hull form models having the lowest friction coefficient would be outliers. However, there are no observations from the tests that these measurements should be considered outliers. To consider these outliers, there should be a constant bias with the measurements with these models. However, there are no evidence from this from the tests, and the same load sensors were used with all the models having simplified hull form. Further research is needed before definitive conclusions can be drawn.

7 Summary/Conclusions

This report presented model-scale measurements in brash ice channel conducted in Aalto University's Aalto Ice and Wave Tank. The measurements included tests with simplified hull forms and a ship model having different friction coefficient in brash ice channels made from common model ice and solid freshwater ice cubes. The tests suggest the friction coefficient correction given in the FSICR guidelines is applicable for hull forms having a vertical bow form (large buttock angle) when those are tested in typical (relatively soft) model ice. On contrary, in a case model-scale testing in brash ice is conducted with solid freshwater ice cubes, the friction coefficient correction given by the rules does not appear directly applicable and further research is needed.

Acknowledgements

The author would like to acknowledge the funding from Winter Navigation Research Board that enabled this work. Furthermore, the author would like to acknowledge the contribution of following persons: Paige Bodnar for the design and construction of the models, Hector Velasquez Reynoso for assisting in 3D printing, Aalto Ice and Wave Tank personnel Otto Puolakka, Teemu Päivärinta and Lasse Turja for assistance in testing and model design and manufacturing, Alice Petry for assistance in model preparation, Sid Oksala, Tim Hammer (TU Delft), and Cody Owen for assisting in the preparation of the ice channel, Riikka Matala (Aker Arctic Technology Oy) for guidance with ice cube channel preparation. Their contribution was essential for this study.

References

Brown, T., Molyneux, D., Williams, C., 1988. Polar 8 Design Phase: With Design D, National Research Council, Institute for Marine Dynamics, Report TR-HYD-29, June 1988.

FSICR, 2019. Guidelines for the Application of the 2017 Finnish-Swedish Ice Class Rules, TRAFI/708629/03.04.01.01/2018, Helsinki, Finland, 8 January 2019.

FSICR, 2021. Ice Class Regulations and the Application Thereof, TRAFICOM/68863/03.04.01.00/2021, Helsinki, Finland, 1 July 2021.

ITTC, 2017. Resistance Tests in Ice, ITTC Recommended Procedures and Guidelines, Section 7.5-02-04-02.1.

ITTC, 2021. Test Methods for Model Ice Properties, ITTC Recommended Procedures and Guidelines, Section 7.5-02-04-02.

Jalonen, R., & Ilves, L., 1990. Experience with a chemically-doped fine-grained model ice. In: Proceedings of the 10th IAHR International Symposium on Ice, pp. 639–651.

Keinonen, A., Browne, R., Revill, C., 1991. Icebreaker Design Synthesis Phase 2: Analysis of contemporary icebreaker performance, Transportation Development Centre, Transport Canada, Report TP 10923 E, September 1991.

Li, F., Suominen, M., Kujala, P., 2021. Ship performance in ice channels narrower than ship beam: Model test and numerical investigation, Ocean Engineering, vol 240, 109922.

Matala, R., Suominen, M., 2022. Investigation of vessel resistance in model scale brash ice channels and comparison to full scale tests, Cold Regions Science and Technology, vol 201, 103617.

Matala, R, Suominen, M, 2023. Scaling principles for model testing in old brash ice channel, Cold Regions Science and Technology, vol 210, 103857.

Mellor, M., 1980. Ship resistance in thick brash ice. Cold Regions Science and Technology, 3 (4), 305–321.

Petry, A., Suominen, M., Matala, R., Skogström, T., Seppänen, E., 2023. Impact of Testing Method on Measured Flexural Strength of Model-Scale Ice,

proceedings of the 27th International Conference on Port and Ocean Engineering under Arctic Conditions, Glasgow, United Kingdom, 12-16 June 2023.

Rehman, A., 2022, Experimental study on friction coefficient correction method for model scale testing in brash ice channel, Master's Thesis, Aalto University, Espoo, Finland, 2022.

Riska, K., 2014. Factors Influencing the Power Requirement in the Finnish-Swedish Ice Class Rules, Winter Navigation Research Board, Report No. 67.

Riska, K., Wilhelmson, M., Englund, K., Leiviskä, T., 1997. Performance of Merchant Vessels in Ice in the Baltic, Winter Navigation Research Board, Report No. 52.